European Journal of Neuroscience: Cognitive Neuroscience

Neural correlates of object size and object location during grasping actions

Simona Monaco[1], Anna Sedda[2], Cristiana Cavina-Pratesi[3] and Jody C. Culham[4]

[1]*Centre for Vision Research, York University, Toronto, Ontario, Canada, M3J 1P3*

[2]*Department of Brain and Behavioural Sciences, University of Pavia, Pavia 27100, Italy*

[3]*Department of Psychology, Durham University, Durham DH1 3LE, United Kingdom*

[4]*Brain and Mind Institute, Department of Psychology, and Neuroscience Program, University of Western Ontario, London, Ontario, Canada, N6A 5B7*

Corresponding Author:
Simona Monaco
Centre for Vision Research
York University
Lassonde Building 009
4700 Keele Street
Toronto, ON, Canada
M3J 1P3
E-mail: simona.monaco@gmail.com
Phone: (+1) 647-8897654

Running title: Size and Location for Grasping

Number of pages	54
Number of figures	4
Number of tables	2
Number of equations	0
Number of words in the manuscript	~8,400
Number of words in the abstract	297
Number of words in the introduction	~610

Keywords: grasping, action, perception, intrinsic, extrinsic, object

Abstract

The visuo-motor channel hypothesis (Jeannerod, *Cognition,* 10 (1-3):135-137, 1981) postulates that grasping movements consist of a grip and a transport component differing in their reliance on intrinsic vs. extrinsic object properties (e.g., size vs. location, respectively). While recent neuroimaging studies have revealed separate brain areas implicated in grip and transport components within the parietal lobe, less is known about the neural processing of extrinsic and intrinsic properties of objects for grasping actions. We used functional magnetic resonance imaging adaptation to examine the cortical areas involved in processing object size, object location or both. Participants grasped (using the dominant right hand) or passively viewed sequential pairs of objects that could differ in size, location or both. We hypothesized that if intrinsic and extrinsic object properties are processed separately, as suggested by the visuo-motor channel hypothesis, we would observe adaptation to object size. On the other hand, if intrinsic and extrinsic object properties are not processed separately, brain ~~a~~reas involved in grasping may show adaptation to both object size and location. We found adaptation to object size for grasping movements in the left anterior intraparietal sulcus, in agreement with the idea that object size is processed separately from location. In addition, the left superior parietal occipital sulcus (SPOC), primary somatosensory and motor area (S1/M1), Precuneus, dorsal premotor cortex (dPM), and supplementary motor area (SMA) showed non-additive adaptation to both object size and location. We propose different roles for aIPS ~~and~~ as compared to SPOC,S1/M1, Precuneus, PMd and SMA. In particular, while aIPS codes intrinsic object properties, which are relevant for hand preshaping and force

scaling, area SPOC,S1/M1, Precuneus, PMd, SMA, and PMd code intrinsic as well as extrinsic object properties, both of which are relevant for digit positioning during grasping.

1. Introduction

The mechanisms underlying grasping movements have been studied for over thirty years. A comprehensive understanding of these mechanisms not only advances explanatory theories about human actions, but also contributes to the development of approaches for robotic grasp that can be used for patients with impaired or lacking motor functions (Chinellato and Del Pobil 2009).

From a behavioral point of view, the visuo-motor channel hypothesis postulated by Jeannerod and colleagues (1981) proposes that grasping movements consist of two components: a grip component relying on intrinsic object properties such as size, and a transport component relying on extrinsic object properties such as location. According to this view, intrinsic and extrinsic object properties are processed independently in separate visual channels.

Recent cognitive neuroscience research has provided evidence in support of separate cortical circuits processing grip and transport for grasping movements. In particular, fMRI and neuropsychology have shown the critical involvement of the anterior intraparietal sulcus (aIPS) and the superior parietal occipital sulcus (SPOC) in processing grip and transport components, respectively (Cavina-Pratesi et al., 2010a, 2010b). A recent transcranial magnetic stimulation (TMS) study corroborated this result and showed causal influence of aIPS in planning the grip component and SPOC in planning the transport component (Vesia et al., 2010, 2013; Tunik et al., 2005). Although these findings reveal the crucial role of the cortical circuits involved in processing the

sensory-motor aspects of grip and transport components for grasping, the extent to which these brain regions also code the intrinsic and extrinsic properties of objects for perception and action remains unknown.

Despite the evidence that grip and transport components are processed separately within aIPS and SPOC, both components are also jointly processed in several other areas within the fronto-parietal grasping network, such as dorsal pre-motor cortex (PMd), supplementary motor area (SMA), primary and secondary somatosensory areas (SI and SII), primary motor area (MI) (Cavina-Pratesi et al., 2010b) and the intraparietal sulcus (IPS) (Konen et al., 2013). In addition, recent neurophysiological studies have shown that neurons in macaque area V6A, the proposed equivalent of human SPOC (Cavina-Pratesi eta l., 2010b), respond not only during reaching movements (Fattori et al., 2001; Galletti et al., 1999) but also code hand posture during grasping (Fattori et al., 2010). Furthermore, recent fMRI studies found that human SPOC could decode grasping vs. reaching actions (Gallivan et al., 2011c, 2013a) and other areas in the dorsal stream, such as PMd and the posterior IPS (pIPS), could also decode between two different grasping movements. Taken together, these findings suggest that grip and transport components are processed separately or in combination in several dorsal stream areas. Are the properties influence them, such as object size and location, also processed in the same manner according to the grasping components that they affect?

Here we used functional magnetic resonance adaptation (fMRA) during grasping and passive viewing to investigate which human brain areas code object size, object

location or both. If intrinsic and extrinsic object properties are indeed processed separately during grasping actions, as suggested by the visuo-motor channel hypothesis, we expected adaptation to object size and location in separate brain regions. In particular, based on our previous findings (Cavina-Pratesi eta l., 2010b), aIPS, thought to processes the grip component, would be expected to adapt to object size (but not location); whereas, SPOC, thought to process the transport component, would be expected to adapt to object location (but not size). Alternatively, if the two properties are integrated, we expected to find no such dissociation. As a control, we also included a passive viewing condition to determine whether effects were specific to grasping actions.

2. Methods

2.1 Participants

Eleven participants (six males and five females, mean age: 32 years old) participated in this study and were financially compensated for their time. All participants were right-handed and had normal or corrected-to-normal visual acuity. This experiment was undertaken with the understanding and written consent of each subject. This study conforms to The Code of Ethics of the World Medical Association (Declaration of Helsinki), printed in the *British Medical Journal* (18 July 1964) and was approved by the Health Sciences Research Ethics Board at the University of Western Ontario.

2.2 Experimental Design

We used an fMRI adaptation paradigm (Grill-Spector et al., 2006) to investigate brain areas involved in processing object size and object location when relevant for reach-to-grasp movements (Figure 1A). On each trial, there was one of four possible combinations of two events (Figure 1B): i) a repetition of both object size and location, ii) a repetition of object size in different locations, iii) a different object size in the same location, iv) a different object size in different locations. These four combinations were factorially crossed with two tasks (Grasp, Look), yielding eight conditions: Grasp:Same Size:Same Location (Grasp SS SL), Grasp:Different Size:Same Location (Grasp DS SL), Grasp:Same Size:Different Location (Grasp SS DL), Grasp:Different Size:Different

Location (Grasp DS DL), Look:Same Size:Same Location (Look SS SL), Look:Different Size:Same Location (Look DS SL), Look:Same Size:Different Location (Look SS DL), Look:Different Size:Different Location (Look DS DL). The task (Grasp or Look) was cued with a verbal instruction at the beginning of each trial. In the "Grasp" condition, participants used the dominant right hand to reach and grasp each of the two objects in the trial sequentially. Specifically, they used the index finger and thumb in a precision grip to grasp the edges of planar shapes without lifting them. Since the starting position of the hand was on the left side of the abdomen (Figure 2A), participants moved the hand to the object by pivoting the forearm at the elbow such that the hand moved along a small arc when reaching to the near object, and along a large arc when reaching to the far object. Therefore, movements towards both near and far objects included transport component with similar directions but different amplitudes. At the end of each event, participants returned the hand to the starting position on the abdomen and kept it still in between trials. In the "Look" (passive viewing) control condition, participants observed the same trial sequences without performing any actions.

INSERT FIGURE 1 ABOUT HERE

INSERT FIGURE 2 ABOUT HERE

This design enabled us to test a major tenet of the visuomotor channels hypothesis – that size and location are represented in separate channels and thus should involve different brain areas. The critical difference between grasp conditions was that the size of the object required an appropriate adjustment of the grip aperture but not of the transport

component, while the location of the object required an appropriate adjustment of the transport component but not of the grip aperture. We hypothesized that brain areas involved in processing object size for the grip component, including aIPS, would show adaptation to size regardless of location while areas processing object location for grasping, including SPOC, would show adaptation to location regardless of size. The look condition served as a control for perceptual differences in object properties and allowed us to determine whether the perception of object size and location is processed in the dorsal stream by the same areas involved in grip and transport component.

In addition to the comparisons between experimental conditions, we also ran an independent functional localizer that allowed us to localize aIPS, SPOC, and a focus in the vicinity of the object-selective lateral occipital complex (LOC), possibly overlapping with the motion-selective middle temporal complex (MT+) (Kourtzi et al., 2001). In each trial, participants performed one of three possible tasks (Grasp, Reach or Look) toward a briefly presented 3D stimulus. Unlike the experimental runs, each trial consisted only of a single presentation of a stimulus. Grasp and Look tasks were similar to those in the experimental runs. In the Reach task participants moved their closed hand towards the object to touch it with the knuckles without forming a grasp.

2.3 Apparatus and Stimuli

The stimuli were presented to the participants on the inclined surface of a black turntable placed above the participant's pelvis (Figure 2A). Each participant lay supine in

the scanner with the head tilted, allowing direct viewing of the stimuli without mirrors. Participants wore headphones to hear audio instructions about the task they were to perform on the upcoming trial. Although the right forearm was free to move, the upper arm was strapped to the bed to be kept still. This helped to avoid artifacts due to the motion of the shoulder and the head (Culham et al., 2003). A detailed description of the apparatus can be found in Monaco et al., 2011

For the experimental runs, we used five different irregular shapes and each shape had a small and a big size (see Fig. 1B for an example). For the independent localizer runs, we used 30 objects whose size was comparable to the size of the small objects used in the experimental runs. The objects were made from white translucent plastic (and manufactured at the University's Machine Services shop). The objects had a constant depth (0.6 cm) but varied in length (from 1.8 to 3.6 cm for the small objects and from 3.25 to 6.5 cm for the big object) and width (from 1.6 to 2.6 for the small objects and from 2.9 to 4.6 cm for the big object). We used different objects across runs but only one object (in the small and big size) within each run to prevent the factor "shape" from interfering with the adaptation effects due to size and location. Indeed, human neuroimaging findings have shown adaptation to object shape in aIPS for grasping (Kroliczak et al., 2008). Therefore, we manipulated digit positions with respect to their absolute location in space rather than to the object (i.e. by changing object shape or orientation).

Except for the two sequentially illuminated presentations of the objects, subjects were in near-complete darkness throughout the length of the trial (only a small dim light was provided by the fixation point). During the inter-trial interval (ITI), and after the participant had performed the first action, the object was quickly replaced and the turntable was rotated by the experimenter. The experimenter even rotated the turntable when the two objects had the same size and location in both events to prevent participants from guessing the characteristics of the second object based on the perceived rotation of the board. Black Velcro markers on the surface guided the experimenter's placement of the objects so the locations and the orientation of the objects were consistent across all trials.

Light emitting diodes (LEDs) were used to provide a fixation point, to illuminate the workspace, and to cue the experimenter about upcoming trials. The participant maintained fixation on an LED positioned approximately 10-15° of visual angle above the objects, so that all objects were presented in the participant's lower visual field. It was not possible to conduct eye tracking during the scan because (1) the set-up time was already considerable; and (2) there are no MR-compatible eye trackers that can monitor gaze in the head-tilted configuration. Nevertheless, in studies where our lab has measured participants' ability to maintain fixation under similar circumstances, they have been able to do so with negligible saccades (Gallivan et al, 2013b) or vergence adjustments (Quinlan & Culham 2007).

A bright LED (illuminator) was used to briefly illuminate the stimulus at the onset of each event of a trial. The illuminator was placed above the participant's head and shone light onto the object. Another set of LEDs was based at the end of the platform, visible to the experimenter but not the participant, to instruct the experimenter about size and location of the objects in the next two events. All of the LEDs were controlled by SuperLab software (Cedrus Corporation, CA) on a laptop PC that received a signal from the MRI scanner at the start of each trial. The windows in the scanner room were blocked and the room lights remained off such that, with the exception of the dim fixation LED which remained on continuously, nothing else in the workspace was visible to the participant when the illuminator LED was off.

For the experimental runs, the object was located near or far relative to the home position of the right hand. The near location was on the left of the fixation while the far location was on the right of fixation. Objects were located along the arc of the right hand reaching trajectory to allow a comfortable grasp, therefore the near object was located about 15-20 degrees below fixation while the far object was located about 10-15 degrees below fixation.

An infrared (IR) camera (MRC Systems GmbH) recorded the performance of each participant for offline investigation of the errors, which were excluded from further analysis (by modeling their activation as a predictor of no interest). The errors were mistakes in the performance of the task (e.g. initiating a grasping movement in a look

condition). Only three trials from all participants were excluded from the analyses due to subject errors.

2.4 Experimental Runs: Timing and Experimental Conditions

We used a slow event-related design (Figure 1A) to prevent contamination of the BOLD response by any potential artifacts generated by the hand movement. Trials were spaced every 22 s to allow the hemodynamic signal to return to baseline between trials (and to allow the experimenter to change the stimulus pairs between trials). Each trial started with the audio cue instructing the participant about the task to be performed. After 2 s (from the onset of the audio cue), the first stimulus was illuminated for 250 ms, cueing the participant to perform the instructed task. The onsets of the first and second events were separated by 4 s, during which the experimenter rotated the turntable to position the second object for the next event. The brief illumination (250 ms) of the second object was the cue for the participant to perform the instructed task a second time. Note that the brief periods of illumination ensured that the participants performed all the actions without visual feedback (that is, in open loop) and reduced the utility and likelihood of saccades to the targets.

Each run consisted of 32 trials and each experimental condition was repeated four times in a random order. A baseline of 16 s was added at the beginning and at the end of each run yielding a run time of approximately 13 minutes per run. Each of the eight possible sequences of object size and locations was evenly distributed through each run.

Sizes and locations occurred equally often within each condition (e.g., the Same Size, Same Location condition had an equal number of trials with Small/Near, Small/Far, Large/Near and Large/Far combinations, though only one combination is shown in Figure 1B). Thus differences between conditions could arise only from the pairing of trials (Different or Same sequence) and not the specific stimuli shown in the conditions. Each participant performed four runs, for a total of 16 trials per experimental condition.

2.5 Independent Functional Localizer: Timing and Experimental Conditions

For the localizer, we used a slow event-related design with one trial every 18 s. A given trial started with the auditory instruction of the task to be performed: Grasp, Reach or Look. After 2 s from the onset of the audio cue, the stimulus was illuminated for 250 ms, cuing the participant to initiate the task. Following the onset of the illumination was a 16 s interval to allow the hemodynamic response to return to baseline before the next trial began. As in the experimental trials, grasping was performed using the index finger and thumb in a precision grip without lifting the object. Each localizer run consisted of 18 trials and each condition was repeated six times in a random order for a run time of approximately 7 minutes. Each participant performed two localizer runs for a total of 12 trials per condition.

2.6 Session Duration

A session for one participant included set-up time (~45 min), 6 functional runs and one anatomical scan, and took approximately 2.5 hours altogether. The experimental runs were performed first, followed by the anatomical scan and the independent functional localizer runs.

2.7 Imaging Parameters

All imaging was performed at the Robarts Research Institute (London, ON, Canada) using a 3 Tesla whole-body MRI system (Siemens Magnetom TIM Trio, Erlangen, Germany). The posterior half of a 12-channel receive only head coil (6-channels) was positioned at the back of the head and tilted at an angle of approximately 30-40 deg; in addition, a 4-channel flex coil was suspended over the forehead (See Figure 2B). Use of the 4-channel flex coil (instead of the anterior six channels of the 12-channel coil) enabled participants to see the stimuli directly while maintaining high signal-to-noise throughout the brain. We collected functional MRI volumes based on the blood oxygenation-level-dependent (BOLD) signal (Ogawa et al., 1992). We used an optimized T2*-weighted single-shot gradient-echo echo-planar imaging (211 mm field of view (FOV) with 64 x 64 matrix size, yielding a resolution of 3.3 mm isovoxel; 3.3 mm slice thickness with no gap; repetition time (TR) = 2 s; echo time (TE) = 30 ms; flip angle (FA) = 78 deg). Each volume comprised 33 slices angled at approximately 30 deg from axial (i.e., approximately parallel to the calcarine sulcus) to sample occipital, parietal, posterior temporal and posterior/superior frontal cortices. The slices were collected in ascending and interleaved order. During each experimental session, a T1-weighted

anatomical reference volume was acquired along the same orientation as the functional images using a 3D acquisition sequence (256 x 240 x 192 FOV with the same matrix size yielding a resolution of 1 mm isovoxel, inversion time, TI = 900 ms, TR = 2300 ms, TE = 5.23 ms, FA = 9 deg).

2.8 Preprocessing

Data were analyzed using Brain Voyager QX software (Brain Innovation 1.10, Maastricht, The Netherlands). Functional data were superimposed on anatomical brain images, aligned on the anterior commissure-posterior commissure line, and transformed into Talairach space (Talairach and Tournoux 1988). Slice time correction with a cubic spline interpolation algorithm was also performed. Functional data from each run were screened for motion or magnet artifacts with cine-loop animation to detect abrupt movements of the head. In addition, we ensured that no obvious motion artifacts (e.g., rims of activation, activation in the ventricles) were present in the activation maps from individual participants. Each functional run was motion corrected using a trilinear/sinc interpolation algorithm, such that each volume was aligned to the volume of the functional scan closest to the anatomical scan. Runs that showed abrupt head motion exceeding 1 mm were discarded from further analyses. Functional data were temporally smoothed to remove frequencies below 2 cycles per run and, for group analyses, also spatially smoothed (full-width, half-maximum, FWHM=6 mm).

2.9 Data Analyses

We performed two types of analyses. First, to investigate brain areas that showed a pattern of results consistent with our predictions we conducted voxelwise group analyses using specific conjunction analyses (see Voxelwise Analyses). For voxelwise group analyses we spatially smoothed data to increase the intersubject overlap in activation foci despite anatomical variability between participants. The voxelwise approach has the advantage that it can identify regions or subregions of activation that were not predicted in advance. Second, to investigate whether the effects were independent of the selection criteria, we performed an analysis using a region of interest (ROI) approach in single subjects by localizing areas typically involved in grasping actions (aIPS, SPOC and LOC/MT+) using an independent set of runs. For the ROI analysis, we used individual data without spatial smoothing. The ROI approach offers the advantages that each area can be identified in individual participants regardless of variations in stereotaxic location and, moreover, specific areas are not blurred with adjacent areas due to inter-individual anatomical variability (Saxe et al., 2006). In addition, because of the *a priori* targeting of certain regions, the ROI approach does not suffer from the drastically reduced statistical power that results from correcting for the very large number of multiple comparisons in a voxelwise approach.

For each participant, we used a general linear model (GLM) that included a predictor for each condition. Each predictor was derived from a rectangular wave function (2 s or 1 volume for the localizer runs; 6 s or 3 volumes for the experimental runs) convolved with a standard double-gamma hemodynamic response function [HRF]

(Brain Voyager QX's default HRF) described in Friston and colleagues (1998). Because the activation for the two events (not to mention the visual presentation and action execution components of each event) overlapped considerably, we modeled them together. That is, in the experimental runs, we chose a time window of 6 s to cover the two sequential presentations of the object and the corresponding actions. Errors in performance were modeled using predictors of no interest. Prior to analysis, the data were %-normalized. The six motion parameters were added as covariates of no interest.

2.10 Statistical Analyses

For each area, we performed five comparisons aimed at testing various hypotheses (see Figure 2B). First, we hypothesized that if object size and location are processed separately, we would observe adaptation effects to these properties in different brain areas. In particular, areas involved in processing object size for grasping, would show adaptation for same vs. different object size, regardless of object location. This would be reflected in adaptation effects in the following comparisons (depicted in Figure 2B): Grasp DS SL vs. Grasp SS SL (comparison 1) and Grasp DS DL vs. Grasp SS DL (comparison 2). In addition, adaptation for Grasp DS DL vs. Grasp SS SL (comparison 5) would not be surprising. On the other hand, areas processing object location would show adaptation for same vs. different object location regardless of size. This pattern would be reflected in adaptation in the following comparisons: Grasp SS DL vs. Grasp SS SL (comparison 3), and Grasp DS DL vs. Grasp DS SL (comparison 4). Second, we hypothesized that areas involved in coding both size and location of an object would

show adaptation when object size and location were repeated (as in the SS SL condition) but not when they were not (as in all the other conditions). This would be reflected in adaptation effects for Grasp DS DL vs. Grasp SS SL (comparison 5), Grasp DS SL vs. Grasp SS SL (comparison 1), Grasp SS DL vs. Grasp SS SL (comparison 3). Activation levels in the conditions Grasp DS SL and Grasp SS DL relative to Grasp DS DL (comparisons 2 and 4) would depend on whether or not the adaptation effects are additive. In particular, additive adaptation effects would be reflected in summation of release from adaptation for Size and Location eliciting the highest response in the DS DL condition, moderate response in DS SL and SS DL conditions, and lowest response in the SS SL condition. Alternatively, non-additive adaptation effects would be reflected in comparable activation levels in all conditions in which either or both object properties changed in subsequent trials, as in the conditions Grasp DS SL, Grasp SS DL, and Grasp DS DL. While the Additive Adaptation effect would suggest that extra processing is needed when both size and location are re-computed in combination as opposed to either one in isolation, the Non-Additive Adaptation effect would suggest that the activation level is independent of the number of object properties being simultaneously processed. Regardless of whether adaptation effects are additive or not, presence of adaptation for repeated vs. novel object size *and* location would reveal processing of both objects properties for grasping.

To examine whether the adaptation effects in the look condition were driven by perceptual processing of object information regardless of action, we performed the same comparisons in the look conditions.

Since our *a priori* hypotheses could be tested using a specific conjunction of comparisons, we chose this approach rather than searching for interaction effects in an analysis of variance (ANOVA). ANOVA main effects and interactions can occur for a variety of reasons other than those hypothesized, making their interpretation less straightforward. For instance, an ANOVA with four factors as in our design (Task, Object Size, Object Location, and Object Size & Location) can potentially give rise to 13 effects, between main effects and interactions, which would be hard to interpret through post-hoc t-tests without any *a priori* hypothesis.

2.11 Voxelwise Analyses

The group random effects (RFX) GLM included one predictor for each of the eight conditions for each participant. Statistical maps were corrected for multiple comparisons using Brain Voyager's cluster-level statistical threshold estimator plug-in (Goebel et al. 2006). This algorithm uses Monte Carlo simulations (1000 iterations) to estimate the probability of a number of contiguous voxels being active purely due to chance while taking into consideration the average smoothness of the statistical maps (Forman et al., 1995). Because map smoothness varies with contrast, different contrasts have different cluster thresholds.

We performed conjunction analyses (Nicols et al., 2005) using the experimental runs to test which brain areas adapted to object size, object location or both object size & location, for grasping tasks (see predictions and contrasts in Figure 2B~~A~~).

In particular, to explore adaptation effects to object Size, we ran a conjunction of the contrasts [(1) AND (2)], while to investigate adaptation effects to object location, we ran a conjunction of the contrasts [(3) AND (4)]. Note that other comparisons would also be expected to be significant, but have not been included because they were not critical to the outlined hypothesis. In order examine adaptation to both size and location we ran a conjunction analysis of [(1) AND (3) AND (5)], which would reveal both Additive and Non-Additive adaptation effects. We further investigated the presence of Additive adaptation effects with the conjunction analysis of [(2) AND (4) AND (5)]. We ran these analyses in the grasp and look conditions, yielding eight conjunction analyses in total.

The minimum cluster size (k) threshold was run for each contrast using an alpha-correction level of 0.05. The highest k-value among the contrasts used in each conjunction analysis was set as the threshold for that analysis. In particular, the cluster thresholds were estimated at 26, 22 and 23 voxels x $(3\ mm)^3$ for a total volume of 702, 594 and 621 mm^3 for each conjunction analysis described in the results (adaptation to size for grasping, adaptation to size for looking, adaptation to both size and location). Areas that did not survive cluster size threshold correction are clearly marked in the figures. Note however that with a conjunction approach, this combination of alpha (p-value) threshold and cluster size (k-value) threshold is actually quite conservative. That is, the

likelihood of two independent contrasts (such as [(1) AND (2)] or [(3) AND (4)]), each with $p < 0.05$, being jointly significant due to chance is $p < (0.05)^2 = 0.0025$. The case for the conjunction contrasts [(1) AND (3) AND (5)] is less clear because they are not fully independent (as each contrast includes the Grasp SS SL condition); nevertheless they require a combination of three rather than two effects so the conjunction probability would be expected to be quite low. Unfortunately, Brain Voyager's cluster-threshold correction does not take joint probabilities into account so we have erred on the conservative side by applying the cluster threshold for a single contrast.

2.12 Region of Interest Analyses

For the independent functional localizer runs, each subject's GLM included three separate predictors: Grasp, Reach, Look. We used these runs to independently identify four ROIs for each participant: the anterior intraparietal area (aIPS), the superior parietal occipital sulcus (SPOC) and the lateral occipital area and/or middle temporal motion complex (LOC/MT+). We localized an aIPS ROI by a comparison of Grasp vs. Reach, a contrast that has been typically used in past studies of this region (Culham et al., 2003). Using the independent functional localizer runs, we localized a SPOC ROI that was defined by a conjunction analysis of [(Grasp > Baseline) AND (Reach > Baseline) AND (Look > Baseline)]. This conjunction analyses is based on robust activation in SPOC to luminance transients (Bristow et al., 2005; Portin et al., 1998; Vanni et al., 2001) and has been used in a recent study to localize the SPOC area (Monaco et al., 2011). The conjunction analyses used to localize SPOC revealed another consistent focus of

activation located at the posterior end of the inferior temporal sulcus that corresponds to anatomical location of LOC/MT+. LO and MT+ can only be distinguished by comparing object-selective and motion-selective localizers (respectively), which were not possible to include here. Moreover, even with such localizers, the two areas show partial overlap (Kourtzi et al., 2001). Given these caveats, we refer to this region as LOC/MT+. Area PMd was localized with a conjunction analyses of [(Grasp > Look) AND (Reach > Look)] based on previous studies showing higher activation for Grasp and Reach vs. Look in PMd (Cavina-Pratesi et al., 2010b; Monaco et al., 2011, 2013).

ROIs were defined using a voxelwise contrast in each individual. For each ROI from each participant, we found the voxel with peak activation near the expected location of the ROI: junction of intraparietal and postcentral sulci for aIPS; superior end of the parietal occipital sulcus for SPOC; junction of inferior temporal sulcus and lateral occipital sulcus for LOC/MT+. Then thresholds for each subject were lowered and a box-shaped ROI of $(10\ mm)^3 = 1000\ mm^3$ centered around the peak voxel was selected. For each ROI from each participant, we extracted the event-related time course of the experimental runs and calculated the percent BOLD signal change (%BSC) at the peak response (1 volume) for further analysis. Subjects that did not show activation in the expected anatomical location were not included in the analyses of the area.

3. Results

3.1 Voxelwise Analyses (Averaged Data)

We performed conjunction analyses using the experimental runs to test which brain areas adapted to object size (comparisons 1 and 2 in Figure 2B), object location (comparisons 3 and 4 in Figure 2B) or both (comparisons 1, 3 and 5 in Figure 2B). Activation maps and bar graphs are shown in Figure 3). Talairach coordinates and the numbers of voxels for each area are reported in Table 1. Comparisons that are not independent of the selection criteria are clearly marked with square brackets.

INSERT FIGURE 3, TABLE 1

The first conjunction analysis [(1) AND (2)] was aimed at examining brain areas that showed adaptation to object size regardless of object location. We performed this conjunction separately for grasp and look conditions and found adaptation to object size, regardless of location, for grasping in area aIPS in the left hemisphere. This was reflected in adaptation for same vs. different size in same location (comparison 1, $p<0.001$) and different location condition (comparison 2, $p=0.002$). In addition, comparison 5, which compared a different size condition (DS DL) to a same-size condition (SS SL), was significant for grasping ($p = 0.002$) and looking ($p=0.015$) conditions. In contrast, area LOC/MT+ in the left hemisphere showed adaptation to object size, regardless of location, for look but not grasp conditions. In particular, there was adaptation for same vs.

different size in same location (comparison 1, $p=0.002$) and different location condition (comparison 2, $p<0.001$). In addition, comparison 5 was significant for look ($p = 0.009$) and grasp conditions ($p=0.041$).

The second conjunction analysis [(3) AND (4)] was performed to investigate which areas showed adaptation to object location regardless of object size. No adaptation effect was revealed by this conjunction analysis for grasp or look conditions ($p>0.05$).

The third conjunction analysis [(1) AND (3) AND (5)] was performed to explore joint adaptation effects to object size and location. This analysis revealed adaptation effects in LH PMd, SMA, LH SPOC, LH Precuneus and LH S1/M1. The same analysis run on looking tasks did not reveal any significant activation. Notably, in none of these areas were voxelwise contrasts (2) or (4) significant ($p>0.05$), suggesting that adaptation effects to object size and location are not additive.

In order to explore whether any area showed an additive adaptation effect for object size and location, we ran the following conjunction analysis in grasping and looking conditions: [(2) AND (4) AND (5)]. These analyses did not reveal any active voxels ($p>0.05$).

3.2 Region of Interest Analyses

We were able to localize SPOC, aIPS and LOC/MT+ in the left hemisphere of ten of eleven participants (not always the same ten). Averaged Talairach coordinates and number of voxels are specified in Table 2. Results for SPOC, aIPS and LOC/MT+ ROIs are shown for each participant in Figure 4.

INSERT FIGURE 4 AND TABLE 2 ABOUT HERE

3.2.1 Anterior Intraparietal Sulcus (aIPS)

The averaged Talairach coordinates for aIPS (see Table 2) are in agreement with previous fMRI experiments for aIPS (Culham et al., 2003; Frey et al., 2005; Castiello and Begliomini 2008; Kroliczak et al., 2007, 2008).

The experimental runs revealed adaptation to object Size in aIPS for grasping in same location conditions (comparison 1, $p=0.029$) as well as in different location conditions (comparison 2, $p=0.039$). In addition, comparison 5, which also compared a different size condition (DS DL) to a same size condition (SS SL) was also significant ($p = 0.017$). The contrast of DS SL vs. SS DL would also be expected to be significant, but had not been included because it was not critical to the hypotheses outlined in Figure 2B.

3.2.2 Lateral Occipital/Middle Temporal Complex (LOC/MT+)

The averaged Talairach coordinates for LOC/MT+ (See Table 2) are in the vicinity of both the LOC and MT+ regions defined by Kourtzi and colleagues (2001) and may include the region of overlap between the two functionally defined regions.

The experimental runs revealed adaptation to object size in LOC/MT+ for looking in same location conditions (comparison 1, $p=0.006$) as well as in different location conditions (comparison 2, $p=0.033$). In addition, comparison 5, which compared a different size condition (DS DL) to a same-size condition (SS SL), was significant for looking ($p=0.002$) and grasping tasks ($p=0.014$). The contrast of DS SL vs. SS DL would also be expected to be significant, but had not been included because it was not critical to the hypotheses outlined in Figure 2B.

3.2.3 Superior Parieto-Occipital Cortex (SPOC)

The averaged Talairach coordinates for SPOC (see Table 2) are in agreement with previous fMRI experiments for SPOC (Culham et al., 2003; Gallivan et al., 2011a, 2011c; Monaco et al., 2011; Quinlan and Culham, 2007) and area V6 (Pitzalis et al., 2006, 2010) and slightly more lateral to the location for SPOC described by Gallivan and colleagues in 2009. The anatomical location of our area fell between the anterior (aSPOC) and posterior (pSPOC) subdivisions described by Cavina-Pratesi and colleagues (2010).

For the experimental runs, left SPOC showed patterns consistent with non-additive adaptation to size and location. In particular, we found adaptation effects in

grasping tasks when object size and location were repeated as opposed to when they were not (comparison 1, p=0.01; comparison 3, p=0.002; comparison 5, p=0.01).

It is worth noting that although aIPS and SPOC failed to survive the cluster-size thresholding in the group data, the pattern of results was identical in the ROI analyses, which do not require correction for multiple comparisons because the regions are defined independently and a priori.

4. Discussion

Our results show three main findings. First, area aIPS, known to be involved in grasping actions, adapts to object size for grasping movements regardless of object location. This finding is consistent with the visuo-motor channel hypothesis put forward by Jeannerod and colleagues in 1981. Second, our results show evidence of processing of both object size and location for grasping in several cortical areas of the grasping network, such as left SPOC,S1/M1, Precuneus, PMd and. In these areas, the combined effects of object size and location were non-additive; that is, the extent of adaptation to both object size and location did not differ from the extent of adaptation to either aspect alone. This evidence suggests a role for these areas in integrating converging aspects of object information in order to compute a motor program for accurate grasping actions. Third, our results extend previous findings about the involvement of ventral stream areas in processing size of 2D images by showing the involvement of area LOC in processing the size of 3D real objects during viewing conditions.

4.1 Adaptation to Object Size in aIPS

We found adaptation to object size for grasping in aIPS, which has been implicated in the execution of grasping actions (Humans: Begliomini et al., 2007a, 2007b; Binkofski et al., 1998; Cavina-Pratesi et al., 2010b; Culham et al., 2003; Frey et al., 2005. Macaques: Gardner et al., 2007; Murata et al., 2000; Asher et al., 2007). Moreover, other results have demonstrated that grip formation can be perturbed by TMS

to aIPS (reviewed in Tunik et al., 2007) regardless of whether or not arm transport is performed (Vesia et al., 2013).

Past research suggests that aIPS codes the size of the grasped object, but has not distinguished whether this coding is independent of object location. Macaque neurophysiology has found that more than half of AIP neurons are tuned for object size during grasping (Murata et al., 2000). Moreover, recent human neuroimaging found that grasping of two object sizes could be decoded in aIPS (although size and location were confounded; Gallivan et al., 2011b). The power of our design is that we are able to conclude not only that aIPS codes object size, but that it does so regardless of object location. Put another way, we have shown that aIPS adapts when object size is repeated, even when the object is at a different location. In addition, the absence of adaptation to object size during look conditions suggests that this effect is not merely driven by the perceptual processing of object size, but rather by the interaction with the object.

So why would only aIPS code object size regardless of location during grasping, unlike the other regions we investigated? We propose three possible explanations. First, by Jeannerod's (1981) proposal, object size may be critical for determining how wide the hand must open (grip aperture) to grasp the object. However, one influential alternative theory from Smeets and Brenner (1999) argues that the explicit computation of object size is not strictly necessary to grasp an object. Rather, this view proposes that grasping an object simply requires determining suitable locations to place the digits (e.g., index finger and thumb in precision grip) and then positioning the digits independently. Not all

evidence supports the alternative view however. For example, this view would not predict that illusory object size would affect grasping following a delay (as reviewed in Goodale and Westwood, 2004). In our experimental design, any region involved in digit placement per se would be expected to show a pattern of non-additive adaptation to both size and location (Figure 2B) because any change in size and/or location requires a recomputation of digit positions. Indeed many areas do show this pattern (as discussed below). However, the finding that aIPS does not show this pattern indicates that size per se in an important variable in its computations.

Second, one likely factor is that object size is highly predictive of object weight, which is necessary to determine the appropriate grip and load forces. That is, heavier objects – typically larger objects – require stronger upward (load) forces to be lifted and stronger pinching (grip) forces to prevent slippage (Johansson & Westling, 1984). Behavioural and neuropsychological research has shown that parietal areas play an important role in the control of precision grip forces (Ehrsson et al., 2001; Li et al., 2007). Specifically, a TMS study has shown that area aIPS is responsible for processing two precision grasping parameters: hand shaping and grip forces (Davare et al., 2007). Although in our study participants did not lift the objects, visual analysis of object size is used to predictively set the grip forces to manipulate objects in relation to their weight (Cole 2008); therefore it is possible that area aIPS processes object size as a critical factor for computing grip forces even when it is not explicitly required. Indeed, a recent neuroimaging study has shown that area aIPS is involved in the computation of grasp-relevant dimensions of objects in conjunction with object size (Monaco et al., 2013). The

coding of object size may be computed within aIPS or may arise from its connections with areas within the ventral stream (Borra et al., 2008; for a review see Grafton et al., 2010). Although object size per se might be irrelevant for digit placement, it becomes a critical factor insofar as it affects object weight. Indeed, it is possible that requiring participants to lift the object after grasping might increase the relevance of cues such as size as opposed to digit positions also in other areas of the grasping network.

Third, adaptation to object size in area aIPS might also be related to the different extent of movement precision required for different object sizes, thus reflecting differences in neural mechanisms depending on the degree of control required by the movement (Grol et al, 2007; Tarantino et al., 2014). Indeed while a fine digit-oriented action control would be required for the small object, a coarse oriented movement would be required for the big object.

4.1 Adaptation to Object Size in LOC/MT+

LOC/MT+ showed evidence of adaptation to 3D object size for looking tasks. Previous studies have demonstrated adaptation to object size in this area with humans (Grill-Spector et al., 1999; Sawamura et al., 2005) as well as macaques (Sawamura et al., 2005). However, 2D images were used in these studies. Neuroimaging studies investigating the processing of 3D object properties in humans for grasping have shown the involvement of this region in processing object shape (Cavina-Pratesi et al., 2007; Kroliczak et al., 2008; Chouinard et al., 2009) and the grasp-relevant dimension of

objects (Monaco et al., 2013). Since size and the grasp-relevant dimension cannot be disentangled in the present study, it is hard to attribute the adaptation effect in LOC/MT+ to one variable vs. the other.

We found clear adaptation to object size in look conditions in LOC/MT+. Our results confirm and extend previous work that examined processing of object size in LOC/MT+ using 2D images (Grill-Spector et al., 1999; Sawamura et al., 2005). Indeed, since recent research has shown that adaptation effects for 2D images may not generalize to real objects (Snow et al., 2012), our finding adds an important piece of information regarding the neural mechanisms underlying the representation of real 3D objects. Although we did not observe significant adaptation specific to object size in grasp conditions, adaptation for SS SL as compared to DS DL was revealed by both ROI and Voxelwise analysis for grasping.

4.2 Adaptation to Object Size and Location

Several dorsal stream areas, typically involved in skillful actions such as a precision grip, show adaptation to object size and location. These areas span parietal (Precuneus, SPOC and S1) to frontal regions (SMA, PMd), demonstrating that a large network of areas is involved in integrating information about object size and location. Interestingly, among these areas, SMA, PMd and S1/M1 have previously been implicated in both grip and transport component of grasping actions (Cavina-Pratesi et al., 2010b). The fact that these areas showed recovery from adaptation whenever size and/or location

changed and digit positions had to be recomputed fits with a role in the processing of digit positions, as suggested by the Smeets and Brenner (1999).

Surprisingly, although activation levels in M1/S1 were near baseline, small but significant adaptation effects were observed in the Look condition. This may be because Look and Grasp trials were randomly interspersed such that even the sight of the objects evoked some level of action-related processing.

We found adaptation to object size and location in an area previously implicated in reaching and grasping actions in macaques (V6A; Fattori et al., 2001, 2005, 2010), as well as in the transport component of grasping actions in humans (SPOC; Cavina-Pratesi et al., 2010b). While it is well known that lesions to area aIPS severely impair grip scaling (Binkofski et al., 1998), Cavina-Pratesi and colleagues (2010a) found that a patient with optic ataxia arising from brain lesions that included SPOC but not aIPS, showed affected grip scaling as a consequence of inaccurate reaching movements. Therefore, grip scaling was unaffected when no reaching component was required. Remarkably, the patient showed larger variability in the landing position of the wrist (and subsequent digit positions on the object) as compared to controls, regardless of the direction of the reaching component.

In light of our results, these neuropsychological findings and previous neuroimaging findings, we suggest that the role of PMd, SMA, Precuneus and SPOC in grasping actions might be related to the coding of object features, such as size, location,

orientation and center of mass that are used to process object contact points for grasping movements. Indeed, a recent study by Gallivan and colleagues (2013) has shown that premotor and posterior parietal areas, such as PMd, vPM, pIPS and middle IPS, share a common neural coding for grasping an object with the hand or with a tool, suggesting an important role of these areas in processing parameters that are used for grasping, regardless of the kinematics and the muscles used to perform the action. In addition, PMd, SPOC and pIPS have previously been shown to process hand orientation for grasping movements (Monaco et al., 2011).

4.3 Caveats to interpreting lack of Adaptation to Object Location

Although the conjunction analysis did not reveal adaptation to object location regardless of object size, we observed adaptation to object location when object size was repeated (comparison 3) but not when it changed (comparison 4) in LH PMd, SMA, LH SPOC, LH Precuneus and LH S1/M1. This suggests that these areas process object location but only insofar as other parameters, like object size, are unchanged. Indeed, a number of studies have shown that these areas do indeed code location (when size is not varied ~~too~~). For example, Gallivan and colleagues (2011b) were able to decode target location for reaching movements using multivoxel pattern analysis (MVPA) in many of the same regions, including SPOC, PMd, and SMA.

One might wonder why we did not see adaptation to location when object size changed (comparison 4) given that many brain areas show a strong preference to

locations in the contralateral hemifield. Here it is important to emphasize that fMRI activation and fMRA likely reflect different aspects of neural processing. Brain activation levels (% signal change) reflect the preference of an area. For example, areas in the left hemisphere may show higher activation for actions in the right side of space. In contrast, fMRA is known to reflect a reduction in neural processing (be it lesser, faster, or more tightly tuned processing; Grill-Spector et al., 2006) that results from repetition of one dimension of a stimulus. An area may show a preference for a contralateral location but not any processing benefit if the location is repeated (particularly in this case if another attribute – size – is also changed). Consideration of these factors can also explain the absence of adaptation to object location in LOC/MT+ despite the well-known preference in LOC/MT+ for stimuli presented in contralateral as opposed to the ipsilateral hemifield (Niemeier et al., 2005; Hemond et al., 2007; Large et al., 2008; McKyton and Zohary 2007).

4.4 Conclusions

To summarize, we found that while object size for grasping movements elicits adaptation in LH aIPS, an area known to be involved in processing the grip component of grasping actions, adaptation to both size and location was observed in several other areas of the fronto-parietal network, such as LH PMd, SMA, LH SPOC, LH Precuneus and LH S1/M1. Taken together, these results suggest that the cortical processing of intrinsic and extrinsic object properties for action does not strictly follow the anatomical segregation

of grip and transport components of a movement. Indeed, these two components are likely integrated to compute accurate grasping movements. We propose different roles for aIPS and other areas in the fronto-parietal network in grasping actions. In particular, we suggest that area aIPS is involved in processing object attributes, such as size and shape, in order to compute information about the object, like its weight, for the execution of an efficient grasp. On the other hand, PMd, SMA, SPOC and Precuneus are involved in the integration of object size and location in order to process the ~~fine~~ digit positioning of the fingers on the object to allow a stable grasp.

Acknowledgements

This research was funded by a grant from the Canadian Institutes of Health Research (MOP84293) to JCC. We thank Adam McLean and Joy Williams for help with data acquisition.

Conflict of Interest or Acknowledgments

The authors have no conflict of interest to declare.

aIPS, anterior intraparietal sulcus

aSPOC, anterior superior parietal occipital cortex

DS DL, Different Size:Different Location

DS SL, Different Size:Same Location

fMRIa, functional magnetic resonance imaging adaptation

LH, left hemisphere

LOC/MT+, lateral occipital complex/middle temporal

S1, primary somatosensory area

M1, primary motor area

pSPOC, posterior superior parietal occipital cortex

SMA, supplementary motor area

SPOC, superior parietal occipital cortex

PMd, dorsal premotor cortex

SS DL, Same Size:Different Location

SS SL, Same Size:Same Location

TMS, transcranial magnetic stimulation

References:

Asher, I., Stark, E., Abeles, M. & Prut, Y. (2007) Comparison of direction and object selectivity of local field potentials and single units in macaque posterior parietal cortex during prehension. J. Neurophysiol., **97**, 3684-3695.

Begliomini, C., Caria, A., Grodd, W. & Castiello, U. (2007) Comparing natural and constrained movements: New insights into the visuomotor control of grasping. PLoS One, **2**, e1108.

Begliomini, C., Wall, M.B., Smith, A.T. & Castiello, U. (2007) Differential cortical activity for precision and whole-hand visually guided grasping in humans. Eur. J. Neurosci., **25**, 1245-1252.

Binkofski, F., Dohle, C., Posse, S., Stephan, K.M., Hefter, H., Seitz, R.J. & Freund, H.J. (1998) Human anterior intraparietal area subserves prehension: A combined lesion and functional MRI activation study. Neurology, **50**, 1253-1259.

Borra, E., Belmalih, A., Calzavara, R., Gerbella, M., Murata, A., Rozzi, S. & Luppino, G. (2008) Cortical connections of the macaque anterior intraparietal (AIP) area. Cereb. Cortex, **18**, 1094-1111.

Bristow, D., Frith, C. & Rees, G. (2005) Two distinct neural effects of blinking on human visual processing. Neuroimage, **27**, 136-145.

Castiello, U. & Begliomini, C. (2008) The cortical control of visually guided grasping. Neuroscientist, **14**, 157-170.

Cavina-Pratesi, C., Ietswaart, M., Humphreys, G.W., Lestou, V. & Milner, A.D. (2010a) Impaired grasping in a patient with optic ataxia: Primary visuomotor deficit or secondary consequence of misreaching? Neuropsychologia, **48**, 226-234.

Cavina-Pratesi, C., Monaco, S., Fattori, P., Galletti, C., McAdam, T.D., Quinlan, D.J., Goodale, M.A. & Culham, J.C. (2010b) Functional magnetic resonance imaging reveals the neural substrates of arm transport and grip formation in reach-to-grasp actions in humans. J. Neurosci., **30**, 10306-10323.

Chinellato, E. & Del Pobil, A.P. (2009) The neuroscience of vision-based grasping: A functional review for computational modeling and bio-inspired robotics. J. Integr. Neurosci., **8**, 223-254.

Chouinard, P. A., Large, M.E., Chang, E.C. & Goodale, M.A. (2009) Dissociable neural mechanisms for determining the perceived heaviness of objects and the predicted weight of objects during lifting: An fMRI investigation of the size-weight illusion. Neuroimage, **44**, 200-212.

Cole, K. J. (2008) Lifting a familiar object: Visual size analysis, not memory for object weight, scales lift force. Exp. Brain Res., **188**, 551-557.

Culham, J. C., Danckert, S.L., DeSouza, J.F., Gati, J.S., Menon, R.S. & Goodale, M.A. (2003) Visually guided grasping produces fMRI activation in dorsal but not ventral stream brain areas. Exp. Brain Res., **153**, 180-189.

Davare, M., Andres, M., Clerget, E., Thonnard, J.L. & Olivier, E. (2007) Temporal dissociation between hand shaping and grip force scaling in the anterior intraparietal area. J. Neurosci., **27**, 3974-3980.

Ehrsson, H. H., Fagergren, E. & Forssberg, H. (2001) Differential fronto-parietal activation depending on force used in a precision grip task: An fMRI study. J. Neurophysiol., **85**, 2613-2623.

Fattori, P., Raos, V., Breveglieri, R., Bosco, A., Marzocchi, N. & Galletti, C. (2010) The dorsomedial pathway is not just for reaching: Grasping neurons in the medial parieto-occipital cortex of the macaque monkey. J. Neurosci., **30**, 342-349.

Fattori, P., Kutz, D.F., Breveglieri, R., Marzocchi, N. & Galletti, C. (2005) Spatial tuning of reaching activity in the medial parieto-occipital cortex (area V6A) of macaque monkey. Eur. J. Neurosci., **22**, 956-972.

Fattori, P., Gamberini, M., Kutz, D.F. & Galletti, C. (2001) 'Arm-reaching' neurons in the parietal area V6A of the macaque monkey. Eur. J. Neurosci., **13**, 2309-2313.

Forman, S. D., Cohen, J.D., Fitzgerald, M., Eddy, W.F., Mintun, M.A. & Noll, D.C. (1995) Improved assessment of significant activation in functional magnetic resonance imaging (fMRI): Use of a cluster-size threshold. Magn. Reson. Med., **33**, 636-647.

Frey, S. H., Vinton, D., Norlund, R. & Grafton, S.T. (2005) Cortical topography of human anterior intraparietal cortex active during visually guided grasping. Brain Res. Cogn. Brain Res., **23**, 397-405.

Friston, K. J., Fletcher, P., Josephs, O., Holmes, A., Rugg, M.D. & Turner, R. (1998) Event-related fMRI: Characterizing differential responses. Neuroimage, **7**, 30-40.

Galletti, C., Fattori, P., Gamberini, M. & Kutz, D.F. (1999) The cortical visual area V6: Brain location and visual topography. Eur. J. Neurosci., **11**, 3922-3936.

Gallivan, J. P., McLean, D.A., Flanagan, J.R. & Culham, J.C. (2013a) Where one hand meets the other: Limb-specific and action-dependent movement plans decoded from preparatory signals in single human frontoparietal brain areas. J. Neurosci., **33**, 1991-2008.

Gallivan, J. P., McLean, D.A., Valyear, K.F. & Culham, J.C. (2013b) Decoding the neural mechanisms of human tool use. Elife, **2**, e00425.

Gallivan, J. P., McLean, A. & Culham, J.C. (2011a) Neuroimaging reveals enhanced activation in a reach-selective brain area for objects located within participants' typical hand workspaces. Neuropsychologia, **49**, 3710-3721.

Gallivan, J. P., McLean, D.A., Smith, F.W. & Culham, J.C. (2011b) Decoding effector-dependent and effector-independent movement intentions from human parieto-frontal brain activity. J. Neurosci., **31**, 17149-17168.

Gallivan, J. P., McLean, D.A., Valyear, K.F., Pettypiece, C.E. & Culham, J.C. (2011c) Decoding action intentions from preparatory brain activity in human parieto-frontal networks. J. Neurosci., **31**, 9599-9610.

Gardner, E. P., Babu, K.S., Ghosh, S., Sherwood, A. & Chen, J. (2007) Neurophysiology of prehension. III. representation of object features in posterior parietal cortex of the macaque monkey. J. Neurophysiol., **98**, 3708-3730.

Goebel, R., Esposito, F. & Formisano, E. (2006) Analysis of functional image analysis contest (FIAC) data with brainvoyager QX: From single-subject to cortically aligned group general linear model analysis and self-organizing group independent component analysis. Hum. Brain Mapp., **27**, 392-401.

Goodale, M. A. & Westwood, D.A. (2004) An evolving view of duplex vision: Separate but interacting cortical pathways for perception and action. Curr. Opin. Neurobiol., **14**, 203-211.

Grafton, S. T. (2010) The cognitive neuroscience of prehension: Recent developments. Exp. Brain Res., **204**, 475-491.

Grill-Spector, K., Henson, R. & Martin, A. (2006) Repetition and the brain: Neural models of stimulus-specific effects. Trends Cogn. Sci., **10**, 14-23.

Grill-Spector, K., Kushnir, T., Edelman, S., Avidan, G., Itzchak, Y. & Malach, R. (1999) Differential processing of objects under various viewing conditions in the human lateral occipital complex. Neuron, **24**, 187-203.

Hemond, C. C., Kanwisher, N.G. & Op de Beeck, H.P. (2007) A preference for contralateral stimuli in human object- and face-selective cortex. PLoS One, **2**, e574.

Jeannerod, M. (1981) Specialized channels for cognitive responses. Cognition, **10**, 135-137.

Johansson, R. S. & Westling, G. (1984) Roles of glabrous skin receptors and sensorimotor memory in automatic control of precision grip when lifting rougher or more slippery objects. Exp. Brain Res., **56**, 550-564.

Konen, C. S., Mruczek, R.E., Montoya, J.L. & Kastner, S. (2013) Functional organization of human posterior parietal cortex: Grasping- and reaching-related activations relative to topographically organized cortex. J. Neurophysiol., **109**, 2897-2908.

Kourtzi, Z. & Kanwisher, N. (2001) Representation of perceived object shape by the human lateral occipital complex. Science, **293**, 1506-1509.

Kroliczak, G., McAdam, T.D., Quinlan, D.J. & Culham, J.C. (2008) The human dorsal stream adapts to real actions and 3D shape processing: A functional magnetic resonance imaging study. J. Neurophysiol., **100**, 2627-2639.

Kroliczak, G., Cavina-Pratesi, C., Goodman, D.A. & Culham, J.C. (2007) What does the brain do when you fake it? an FMRI study of pantomimed and real grasping. J. Neurophysiol., **97**, 2410-2422.

Large, M. E., Culham, J., Kuchinad, A., Aldcroft, A. & Vilis, T. (2008) fMRI reveals greater within- than between-hemifield integration in the human lateral occipital cortex. Eur. J. Neurosci., **27**, 3299-3309.

Li, Y., Randerath, J., Goldenberg, G. & Hermsdorfer, J. (2007) Grip forces isolated from knowledge about object properties following a left parietal lesion. Neurosci. Lett., **426**, 187-191.

McKyton, A. & Zohary, E. (2007) Beyond retinotopic mapping: The spatial representation of objects in the human lateral occipital complex. Cereb. Cortex, **17**, 1164-1172.

Monaco, S., Cheng, Y., Medendorp, P.W., Crawford, J.D., Fiehler, K. & Henriques, Y.P.D. (2013) Functional magnetic resonance imaging adaptation reveals the cortical networks for processing grasp-relevant object properties. Cereb. Cortex, **doi: 10.1093/cercor/bht006**.

Monaco, S., Cavina-Pratesi, C., Sedda, A., Fattori, P., Galletti, C. & Culham, J.C. (2011) Functional magnetic resonance adaptation reveals the involvement of the dorsomedial stream in hand orientation for grasping. J. Neurophysiol., **106**, 2248-2263.

Murata, A., Gallese, V., Luppino, G., Kaseda, M. & Sakata, H. (2000) Selectivity for the shape, size, and orientation of objects for grasping in neurons of monkey parietal area AIP. J. Neurophysiol., **83**, 2580-2601.

Nichols, T., Brett, M., Andersson, J., Wager, T. & Poline, J.B. (2005) Valid conjunction inference with the minimum statistic. Neuroimage, **25**, 653-660.

Niemeier, M., Goltz, H.C., Kuchinad, A., Tweed, D.B. & Vilis, T. (2005) A contralateral preference in the lateral occipital area: Sensory and attentional mechanisms. Cereb. Cortex, **15**, 325-331.

Portin, K., Salenius, S., Salmelin, R. & Hari, R. (1998) Activation of the human occipital and parietal cortex by pattern and luminance stimuli: Neuromagnetic measurements. Cereb. Cortex, **8**, 253-260.

Quinlan, D. J. & Culham, J.C. (2007) fMRI reveals a preference for near viewing in the human parieto-occipital cortex. Neuroimage, **36**, 167-187.

Sawamura, H., Georgieva, S., Vogels, R., Vanduffel, W. & Orban, G.A. (2005) Using functional magnetic resonance imaging to assess adaptation and size invariance of shape processing by humans and monkeys. J. Neurosci., **25**, 4294-4306.

Saxe, R., Brett, M. & Kanwisher, N. (2006) Divide and conquer: A defense of functional localizers. Neuroimage, **30**, 1088-96; discussion 1097-9.

Smeets, J. B. & Brenner, E. (1999) A new view on grasping. Motor Control, **3**, 237-271.

Snow, J. C., Pettypiece, C.E., McAdam, T.D., McLean, A.D., Stroman, P.W., Goodale, M.A. & Culham, J.C. (2011) Bringing the real world into the fMRI scanner: Repetition effects for pictures versus real objects. Sci. Rep., **1**, 130.

Tarantino, V., De Sanctis, T., Straulino, E., Begliomini, C. & Castiello, U. (2014) Object size modulates fronto-parietal activity during reaching movements. Eur. J. Neurosci., **39**, 1528-1537.

Tunik, E., Rice, N.J., Hamilton, A. & Grafton, S.T. (2007) Beyond grasping: Representation of action in human anterior intraparietal sulcus. Neuroimage, **36 Suppl 2**, T77-86.

Vanni, S., Tanskanen, T., Seppa, M., Uutela, K. & Hari, R. (2001) Coinciding early activation of the human primary visual cortex and anteromedial cuneus. Proc. Natl. Acad. Sci. U. S. A., **98**, 2776-2780.

Vesia, M., Bolton, D.A., Mochizuki, G. & Staines, W.R. (2013) Human parietal and primary motor cortical interactions are selectively modulated during the transport and grip formation of goal-directed hand actions. Neuropsychologia, **51**, 410-417.

Vesia, M., Prime, S.L., Yan, X., Sergio, L.E. & Crawford, J.D. (2010) Specificity of human parietal saccade and reach regions during transcranial magnetic stimulation. J. Neurosci., **30**, 13053-13065.

Table 1: Talairach coordinates and number of voxels for brain areas showing adaptation effects in the voxelwise group analysis.

Brain areas	Talairach			Vol. (mm^3)
	X	Y	Z	
PMd	-24	-18	64	461
SMA	2	-13	50	367
LH SPOC	-13	-85	27	151
LH Precuneus	-18	-68	48	419
LH S1/M1	-30	-31	56	493
LH aIPS	-53	-41	38	301
LH LOC/MT+	-43	-67	-7	283

Table 2: Average Talairach coordinates and statistical details for aIPS and SPOC in the ROI analysis

Brain areas	Average Talairach coordinates			Average cluster size (mm^3)
	x	y	z	
LH aIPS (10 participants)	-45	-36	45	866
LH LOC/MT+ (10 participants)	43	-71	-10	348
LH SPOC (10 participants)	-12	-83	31	768

Talairach coordinates and numbers of voxels have been averaged across participants. aIPS = anterior intraparietal area; LOC/MT+ = lateral occipital/middle temporal complex; SPOC = superior parieto-occipital area; PMd = dorsal premotor area. LH = left hemisphere; RH = right hemisphere.

Figure legend

Figure 1. Schematic illustration of the experimental design. A) Schematic timing of one trial: before each pair of events, an auditory cue instructed the participant about the upcoming task to be performed ("Grasp", or "Look"). After 2 s, the first object was illuminated for 250 ms, cueing the participant to perform the cued action on the first object. Following 4 s after the first presentation, a second object was illuminated, cuing the participant to perform the same task for the second object. We used an intertrial interval of 16 s. **B)** For each task (Grasp and Look) each pair of sequential events involved one of four possible combinations: i) a repetition of object size and location (upper left panel), ii) a repetition of object size in different locations (lower left panel), iii) a different object size in the same location (upper right panel), iv) a different object size in different locations (lower right panel). Importantly, digit positions were repeated when object size and location were repeated, but not in any other condition. The arrows represent the approximate trajectory of the hand to reach and grasp the object in the grasping tasks. The Look condition served as a control for the visual changes between the objects, therefore no movement was required. The white cross indicates the fixation point. Although only one exemplar trial is shown here, across all trials, for each condition the two object sizes and two spatial locations occurred with equal frequency.

Figure 2. Schematic illustration of the setup. A) The setup required participants to maintain direct gaze at the fixation point (FP, marked with a white cross) throughout each

run. An illuminator LED was used to illuminate the stimuli and an infrared-sensitive camera (IR cam) was used to record the participant's performance in the dark. The home position (HP) of the hand was on the right side of the abdomen. S: same; D: different; G: grasp; L: look. **B)** Statistical comparisons performed to test our hypotheses. Processing of object size would be reflected in adaptation for comparisons 1 and 2 (first panel from left); processing of object location would be reflected in adaptation for comparisons 3 and 4 (second panel from left); processing of object size and location would be reflected in adaptation for comparisons 1, 3 and 5; this adaptation effect could be additive as in comparisons 2 and 4 (third panel from left) or non-additive (first panel from right).

Figure 3. Voxelwise statistical activation maps for regions showing adaptation to object size, object location or both. A) Orange maps show areas with significant adaptation to object size and location for grasping. Green maps show areas with significant adaptation to object size for grasping. Blue maps show areas with significant adaptation to object size for looking ($F > 2.6$, $k = 702$, 594 and 621 mm^3, respectively). Each type of adaptation was defined by a conjunction of contrasts as detailed in Figure **2B~~A~~)** For each area, the bar graphs show the β weights in the eight conditions. Error bars indicate 95% confidence intervals. SPOC, superior parietal occipital cortex; SMA, supplementary motor area; S1, primary somatosensory area; M1, primary motor area; PMd, dorsal premotor cortex; aIPS, anterior intraparietal sulcus; LOC/MT+, lateral occipital complex, LH, left hemisphere; The triangle indicates areas that did not survive the cluster threshold correction (which may have been rather conservative because cluster thresholds only took into account the p value used for a single map ($p < 0.05$) and not the

joint probabilities that arise from conjunction analyses). Note that the statistical contrasts indicated in the bar graphs and marked with square brackets are not independent from the criteria used to define the regions; they are simply included to illustrate that the patterns were seen in the expected conditions but not others (e.g., for grasping but not looking).

Figure 4. Individual statistical maps and activation levels across conditions for the region-of-interest analysis. The ROIs (highlighted by a yellow arrow) were identified in 10 out of 11 participants using the independent functional localizer runs. **A)** Areas SPOC and LOC/MT+ are shown in a sagittal slice while aIPS is shown in a transverse slice for each participant. **B)** The bar graphs display the peak activation (%BSC) in the eight conditions. Error bars indicate 95% confidence intervals. Because the contrasts used to identify each area in each individual came from localizer runs (rather than the experimental runs), the statistical contrasts indicated in the bar graphs are independent from the criteria used to define the regions.

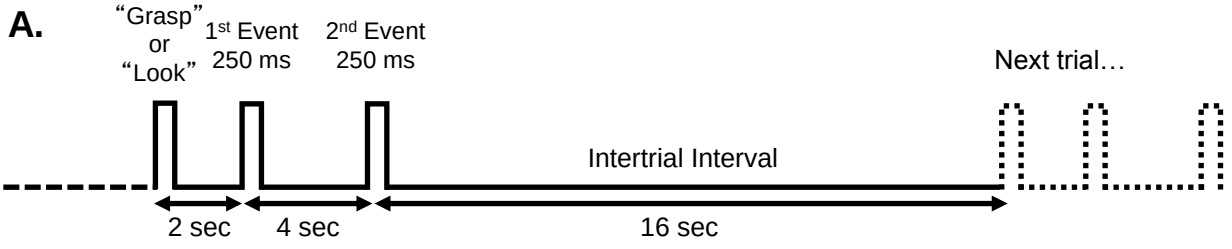
A.
"Grasp" or "Look"
1st Event 250 ms
2nd Event 250 ms
Next trial…
Intertrial Interval
2 sec
4 sec
16 sec

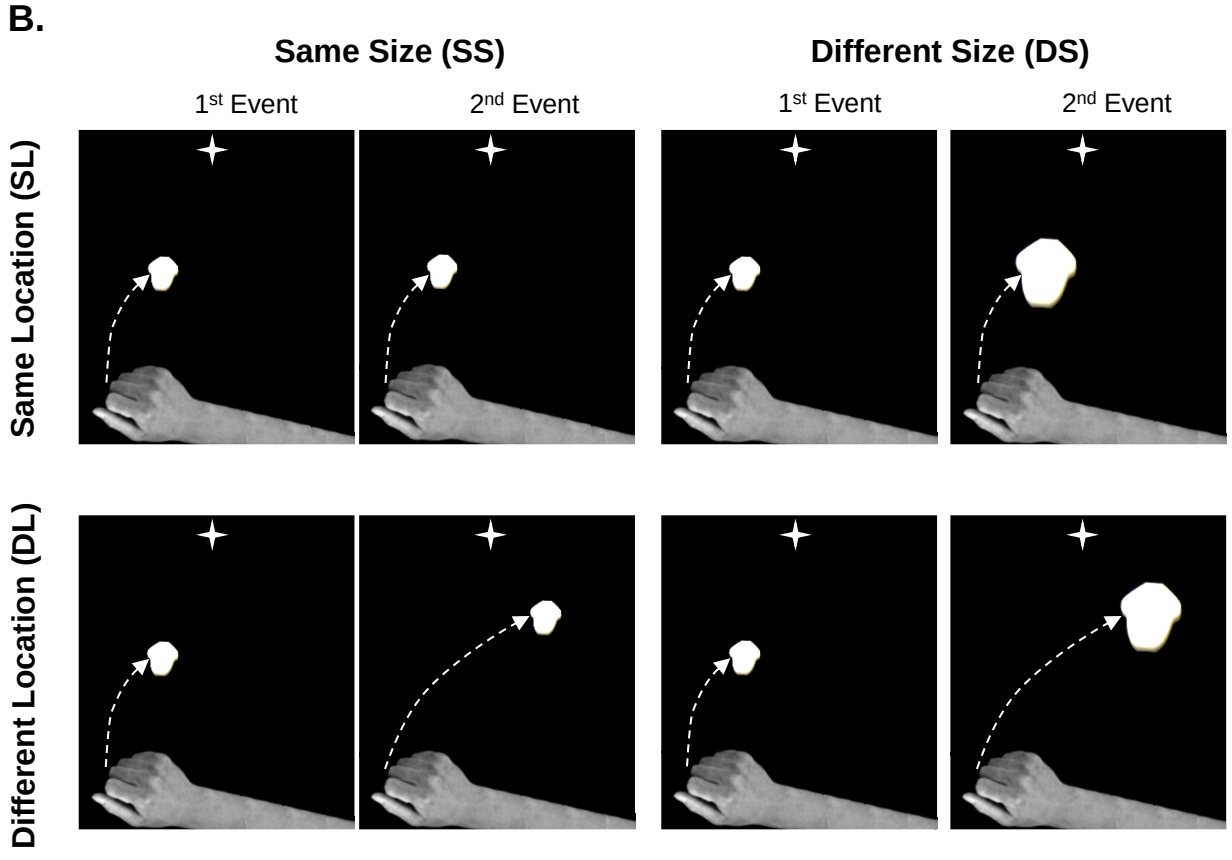
B.
Same Size (SS)
Different Size (DS)
1st Event
2nd Event
1st Event
2nd Event
Same Location (SL)
Different Location (DL)

A.

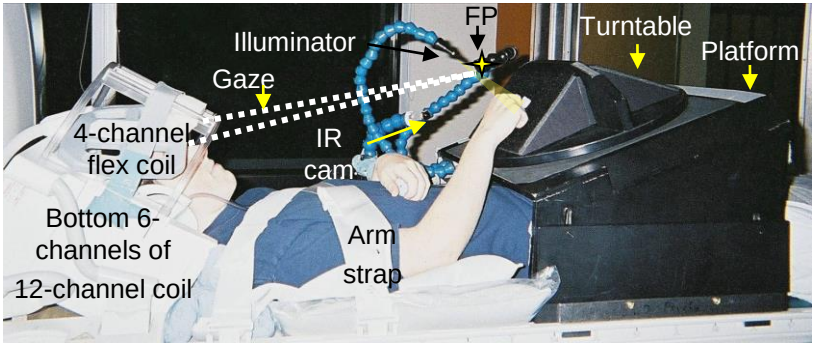
Illuminator
FP
Turntable
Platform
Gaze
4-channel
flex coil
IR
cam
Bottom 6-
channels of
12-channel coil
Arm
strap

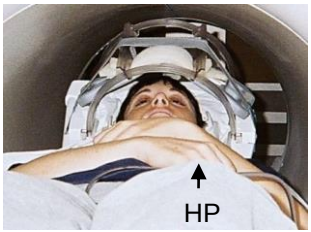
HP

B.

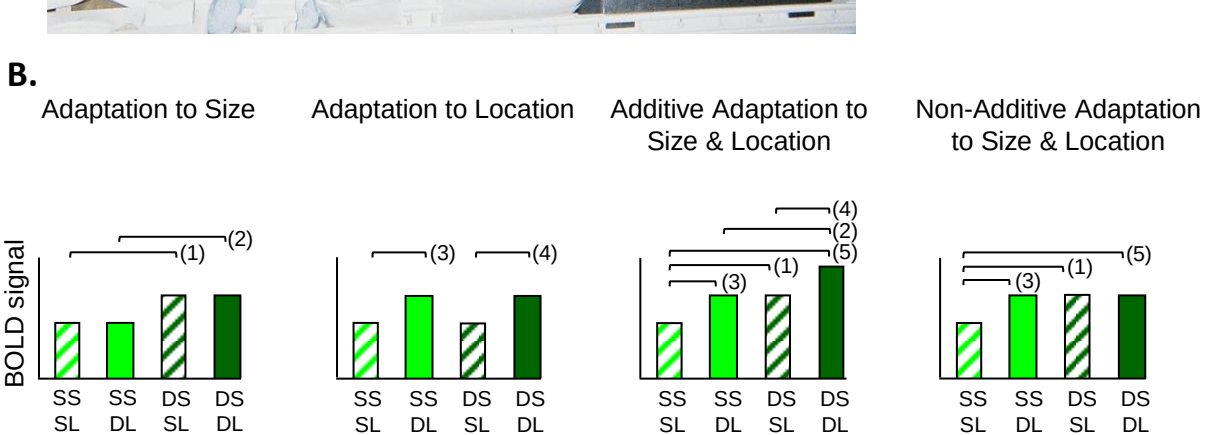
Adaptation to Size
Adaptation to Location
Additive Adaptation to
Size & Location
Non-Additive Adaptation
to Size & Location
BOLD signal
(1)
(2)
(3)
(4)
(5)
SS
SL
SS
DL
DS
SL
DS
DL

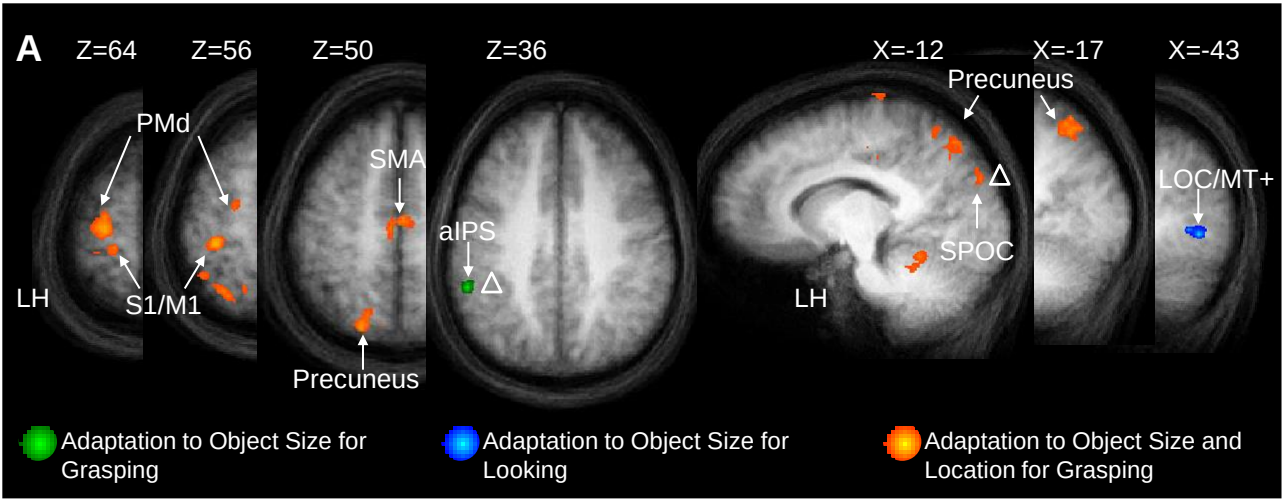
A
Z=64
Z=56
Z=50
Z=36
X=-12
X=-17
X=-43
PMd
SMA
aIPS
Precuneus
SPOC
LOC/MT+
LH
S1/M1
Adaptation to Object Size for Grasping
Adaptation to Object Size for Looking
Adaptation to Object Size and Location for Grasping

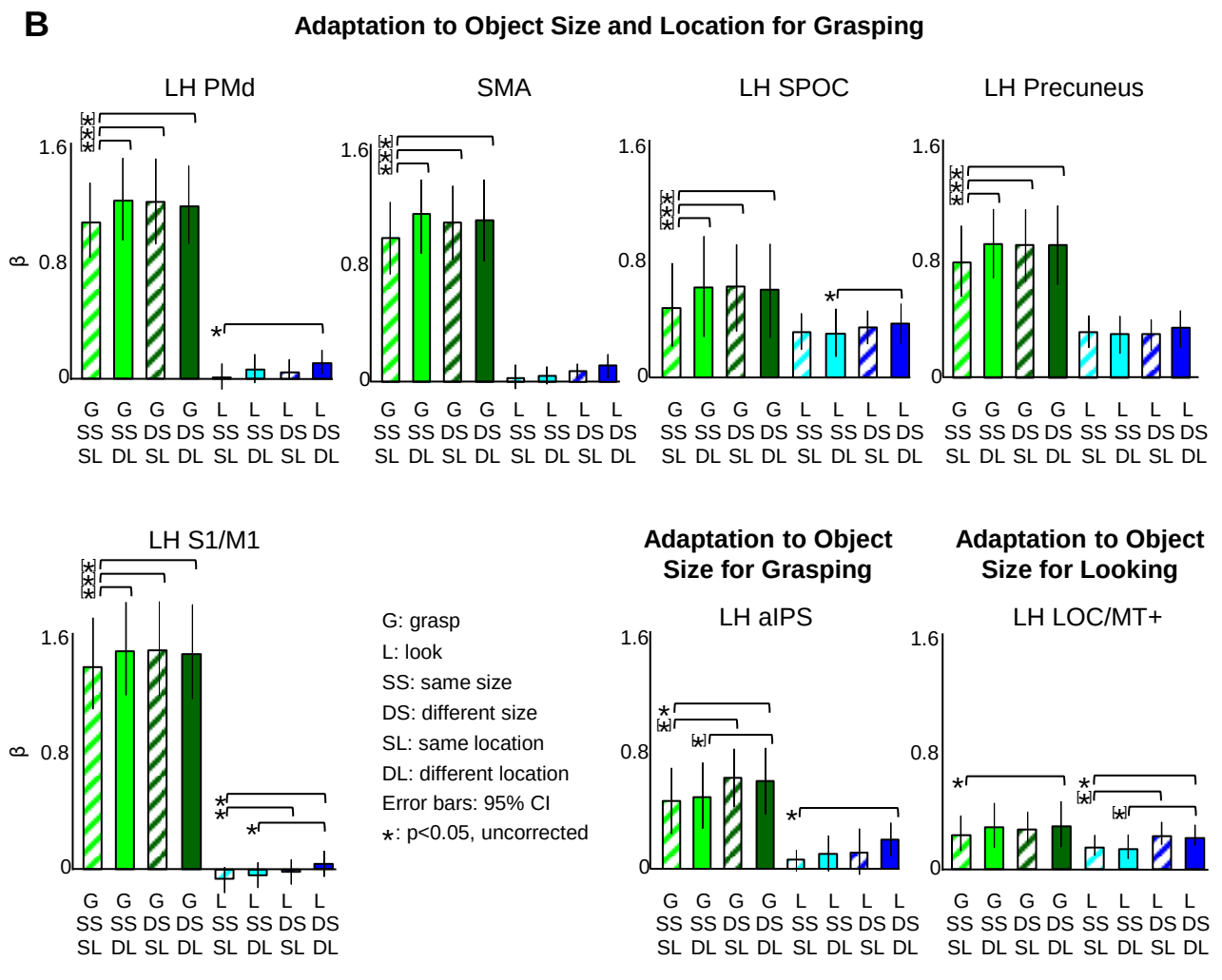
B
Adaptation to Object Size and Location for Grasping
LH PMd
SMA
LH SPOC
LH Precuneus
LH S1/M1
β
1.6
0.8
0
G SS SL
G SS DL
G DS SL
G DS DL
L SS SL
L SS DL
L DS SL
L DS DL
G: grasp
L: look
SS: same size
DS: different size
SL: same location
DL: different location
Error bars: 95% CI
*: p<0.05, uncorrected
Adaptation to Object Size for Grasping
LH aIPS
Adaptation to Object Size for Looking
LH LOC/MT+

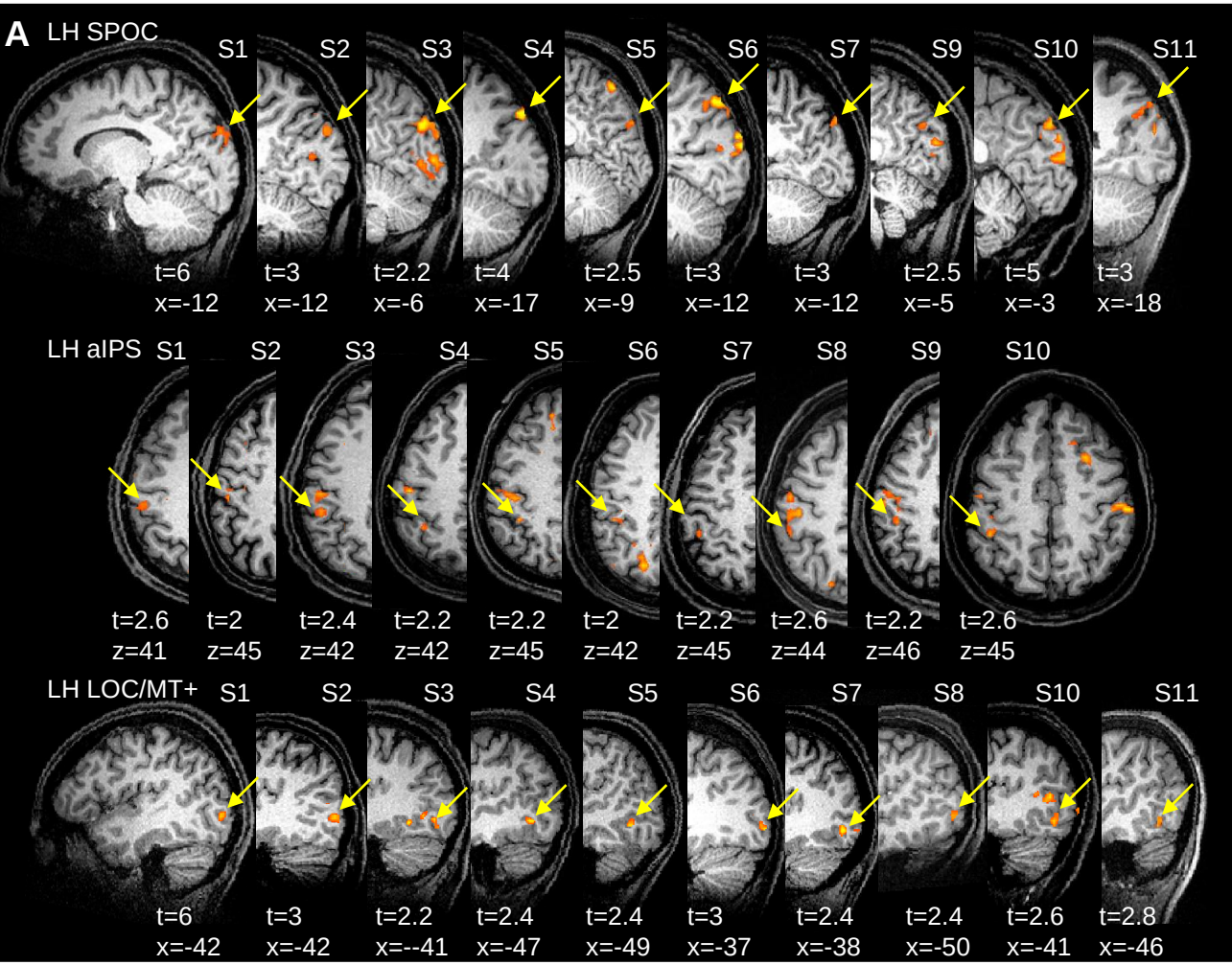
A
LH SPOC
S1 S2 S3 S4 S5 S6 S7 S9 S10 S11
t=6 x=-12
t=3 x=-12
t=2.2 x=-6
t=4 x=-17
t=2.5 x=-9
t=3 x=-12
t=3 x=-12
t=2.5 x=-5
t=5 x=-3
t=3 x=-18
LH aIPS
S1 S2 S3 S4 S5 S6 S7 S8 S9 S10
t=2.6 z=41
t=2 z=45
t=2.4 z=42
t=2.2 z=42
t=2.2 z=45
t=2 z=42
t=2.2 z=45
t=2.6 z=44
t=2.2 z=46
t=2.6 z=45
LH LOC/MT+
S1 S2 S3 S4 S5 S6 S7 S8 S10 S11
t=6 x=-42
t=3 x=-42
t=2.2 x=--41
t=2.4 x=-47
t=2.4 x=-49
t=3 x=-37
t=2.4 x=-38
t=2.4 x=-50
t=2.6 x=-41
t=2.8 x=-46

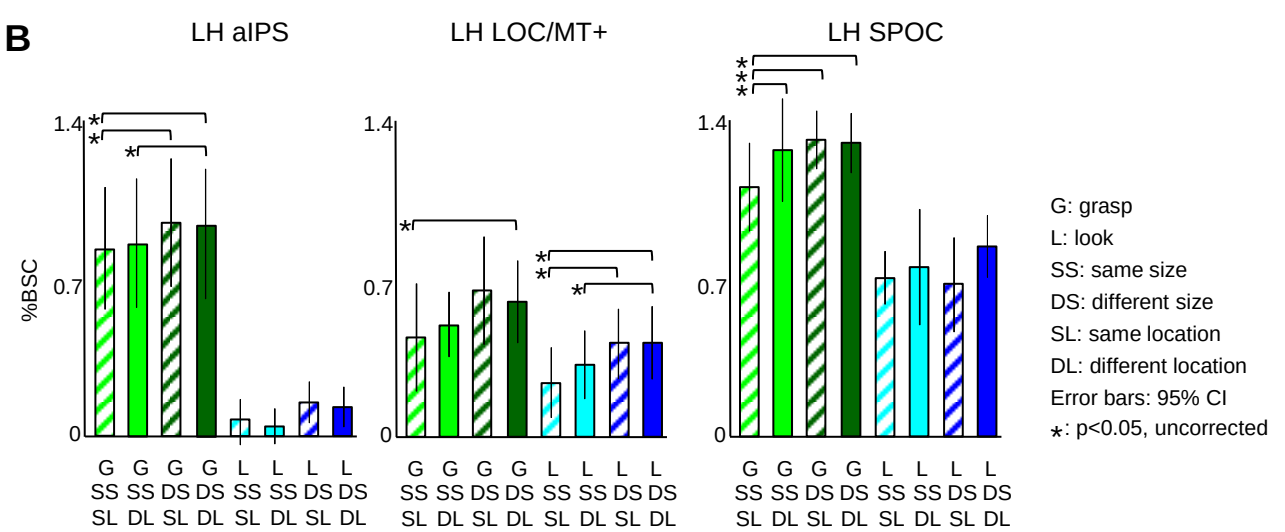
B
LH aIPS
LH LOC/MT+
LH SPOC
%BSC
1.4
0.7
0
G SS SL
G SS DL
G DS SL
G DS DL
L SS SL
L SS DL
L DS SL
L DS DL
G: grasp
L: look
SS: same size
DS: different size
SL: same location
DL: different location
Error bars: 95% CI
*: p<0.05, uncorrected